Korean J. Chem. Eng., **25**(6), 1377-1384 (2008)

Effect of reduction temperature on the preparation of zero-valent iron aerogels for trichloroethylene dechlorination

Jihye Ryu, Dong Jin Suh*, Young-Kwon Park**, and Young-Woong Suh*,†**

*Clean Energy Research Center, Korea Institute of Science and Technology, Seoul 136-791, Korea
**Faculty of Environmental Engineering, University of Seoul, Seoul 130-743, Korea
(*Received 7 January 2008 • accepted 27 April 2008*)

Abstract−Zero-valent iron (ZVI) aerogels have been synthesized by sol-gel method and supercritical CO_2 drying, followed by H_2 reduction in the temperature range of 350-500 °C. When applied to trichloroethylene (TCE) dechlorination, the ZVI aerogel reduced at 370 °C showed the highest performance in the conditions employed in this study. Thus, the effect of reduction temperature in preparing ZVI aerogels has been investigated by several characterizations such as BET, XRD, TPR, and TEM analyses. As the reduction temperature decreased from 500 to 350 °C, the BET surface area of the resulting aerogels increased from 6 to 30 m^2/g, whereas their Fe^0 content decreased up to 64%. It was also found that H_2 reduction at low temperatures such as 350 and 370 °C leads to the formation of ZVI aerogel particles consisting of both Fe^0 and FeO_x in the particle cores with a different amount ratio, where FeO_x is a mixture of maghemite and magnetite. It is, therefore, suggested that reduction at 370 °C for ZVI aerogel preparation yielded particles homogeneously composed of Fe^0 and FeO_x in the amount ratio of 87/13, resulting in high TCE dechlorination rate. On the other hand, when Pd- and Ni-ZVI aerogels were prepared via cogellation and then applied for TCE dechlorination, we also observed a similar effect of reduction temperature. However, the reduction at 350 or 370 °C produced Pd- or Ni-ZVI aerogel particles in which Fe^0 and Fe_3O_4 co-exist homogeneously. Since both Fe^0 and Fe_3O_4 are advantageous in TCE dechlorination, the activities of Pd- and Ni-ZVI aerogels reduced at 350 °C were comparable to those of both aerogels reduced at 370 °C, although the former aerogels have less Fe^0 content.

Key words: Zero-valent Iron, Aerogel, Dechlorination, Trichloroethylene, Thermal Reduction

INTRODUCTION

Chlorinated organic compounds, which are most commonly detected in surface water, groundwater, and soil, are persistent to natural degradation. Various technologies have been explored for removal of chlorinated compounds, including bioremediation, thermal treatment, permeable reactive barriers, etc. One cost-effective method for remediation of contaminated groundwater is the installation of permeable reactive zones or barriers within aquifers [1,2], where zero-valent metals (ZVM) have played a crucial role in reduction of chlorinated organic compounds, toxic metals, and harmful ionic species due to their ability to undergo electron-transfer reactions [3]. Among various metals which have proven to be effective in this application, zero-valent iron (ZVI; Fe^0) particle is widely considered to be one of the most active catalysts in terms of the cost, reduction efficiency, and environmentally benign impact. Such ZVI particles to directly supply electrons for reduction have been applied to the reductive dechlorination of a wide range of environmental pollutants including polychlorinated biphenyls (PCBs), tetrachlorinated ethylene (PCE), and trichloroethylene (TCE), or to the reduction of water-soluble metal ions such as Cr^{6+}, Pb^{2+}, TcO_4^-, etc [4,5]. Among them, TCE is the most frequently targeted probe molecule since more toxic compounds such as dichloroethylene (DCE) isomers and vinyl chloride (VC) rather than the parent compound were produced through the ZVI-promoted reduction [6].

†To whom correspondence should be addressed.
E-mail: ywsuh@kist.re.kr

However, the commercial ZVI samples have been found to show a low rate in TCE dechlorination due to their micro-sized particles. Since the reaction on Fe^0-based particles is a surface-mediated process, the TCE dechlorination rate strongly depends on the surface area of ZVI particles. Hence, a large number of researches have been focused on increasing the surface area of ZVI particles to enhance the reaction rate. To achieve this goal, nano-sized ZVI particles have been variously prepared, typically by a reductive precipitation of iron salts with $NaBH_4$ (ZVI^{BH}) [7]. It has been reported that such nanoparticles with a broad size distribution of 1-100 nm showed a BET surface area of ~33.5 m^2/g, which leads to much higher TCE dechlorination rate than the micro-sized ZVI particles [8]. The as-received samples of ZVI^{BH} were, in addition, shown to consist of a metal core, a thin iron oxide layer, and an outer layer that is mostly oxidized B (borate) with some reduced B (boride), as reported in the literature [9-12]. However, the role of the B-rich shell in ZVI^{BH} samples is still ambiguous, although the activities of ZVI^{BH} samples are greater than those of H_2-reduced ZVI samples for CCl_4 dechlorination in terms of the mass-normalized rate constant [8].

Recently, nano-sized ZVI particles could be prepared by reduction of goethite particles with H_2 at high temperatures of 200-600 °C, followed by allowing the iron particles to stand in water for up to 30 days, yielding the BET surface are of 5-60 m^2/g [13]. These particles (ZVI^{H2}), supplied by Toda Kogyo Corp., were also known to be a two-phase material consisting of α-Fe^0 in the core and Fe_3O_4 in the shell [8,13], where the magnetite layer at the surface of particles can protect inside Fe, resulting in the prolonged catalytic ac-

tivity. Since the activity of ZVI particles is, in general, gradually deteriorated by oxidation of iron metal at their surface, the properties of ZVI[tf2] particles appear to be unique for the TCE degradation.

On the other hand, the iron oxide layer is produced at the ZVI surface by Fe^0 oxidation in aqueous system due to the thermodynamic instability of ZVI: the electrons released by Eq. (1) can produce H_2 and OH^- (Eq. (2)), so that the pH value is getting higher [14]. The consequent rise in pH can precipitate ferrous hydroxide, as shown in Eq. (3). This hydroxide is thermodynamically unstable and can be further oxidized to form magnetite (Fe_3O_4) according to Eq. (4) [15].

$$Fe^0 \rightarrow Fe^{2+} + 2e^- \quad (1)$$

$$2H_2O + 2e^- \rightarrow H_2 + 2OH^-_{(aq)} \quad (2)$$

$$Fe^{2+} + 2OH^- \rightarrow Fe(OH)_{2(s)} \quad (3)$$

$$Fe(OH)_{2(s)} \rightarrow Fe_3O_{4(s)} + H_{2(g)} + 2H_2O \quad (4)$$

The resulting magnetite, which is electrically conductive, can transfer a charge through the interface oxide and, in turn, induce reductive dechlorination, although the degradation rate is lower because the charge transfer rate through the oxide is slower than on a exposed metal surface [16-18]. As the precipitate ages with time, Fe_3O_4 is oxidized to form non electron-conducting maghemite (γ-Fe_2O_3) at the inner layer of the Fe_3O_4 film with a neutral pH, which interferes with electron transfer from the Fe^0 core and then inhibits the redox reaction [16].

Considering the above-mentioned physical properties of nano-sized ZVI required for TCE dechlorination, one could anticipate that the catalytic activity could be maintained and/or enhanced by using the ZVI sample with high surface area consisting of the iron-rich core and the Fe_3O_4-rich shell. In this study, we have utilized a synthetic method of aerogels which are well known to show a high specific surface area and well-developed mesoporosity. To render Fe_3O_4 exist in ZVI aerogel particles, thermal reduction by H_2 was also carried out at temperatures lower than 400 °C. The resulting ZVI aerogels were applied to the dechlorination of TCE at 20 °C, where the effect of reduction temperature on the preparation of ZVI aerogels has been investigated. Also, a similar study was performed using Pd- and Ni-incorporated ZVI aerogels synthesized via cogellation, since nano-sized Pd- and Ni-containing ZVI particles could enhance the dechlorination rate and simultaneously prevent the production of chlorinated intermediates [6,19,20].

EXPERIMENTAL

1. Preparation of ZVI Aerogel

Iron oxide aerogel was synthesized by the sol-gel method and supercritical CO_2 drying, which is similar to the literature method [21]. For preparing iron oxide wet gel, iron chloride hexahydrate ($FeCl_3 \cdot 6H_2O$, Sigma-Aldrich, >98%) was first dissolved in 35 mL of ethanol (Merck, 99.9%) to make a 0.35 M of iron solution. After stirring for 1 h, distilled water was added for the hydrolysis, followed by stirring for another 1 h. To this solution, propylene oxide (Sigma-Aldrich, 99%) as a gelation promoter was added dropwise by a syringe pump at a rate of 1 mL/min with stirring. Then, the molar ratio of $FeCl_3 \cdot 6H_2O$, water, propylene oxide, and ethanol in all samples was 1 : 3 : 7 : 49. During the gel formation, the solution color gradually changed from reddish brown to dark brown while the viscosity increased with heat evolving. The ethanol solvent in wet gels was then exchanged with supercritical CO_2 for 3-4 h at a pressure of 3,000 psi at 60 °C.

The resulting iron oxide aerogel was reduced in 5% H_2/Ar at a flow rate of 400 mL/min by ramping the temperature with 1 °C/min to the desired temperature in the range of 350-500 °C and holding for 2 h. Finally, ZVI aerogels were obtained after a treatment in 1% O_2/N_2 at a flow of 60 mL/min for 1 h at room temperature, due to the pyrophoric character of iron. The physical properties of ZVI aerogels reduced at different temperatures are summarized in Table 1 (entries 1-4), where the number in aerogel samples' name stands for the reduction temperature.

2. Preparation of Pd- and Ni-ZVI Aerogels

Palladium- or nickel-containing iron oxide aerogel was prepared by the same procedure as the ZVI aerogel, except that palladium

Table 1. Physical properties of ZVI, Pd- and Ni-ZVI aerogels reduced at various temperatures

Entry	Sample name	Reduction temperature (°C)	BET surface area (m^2/g)	Total pore volume (cm^3/g)	Average pore diameter (nm)	Fe^0 content[a] (mol%)
1	ZVI-350	350	30	0.284	33.05	64
2	ZVI-370	370	25	0.147	22.34	87
3	ZVI-400	400	19	0.045	9.07	99
4	ZVI-500	500	6	n.d.[b]	n.d.[b]	100
5	Pd-ZVI-350	350	21	0.102	19.64	78
6	Pd-ZVI-370	370	18	0.066	15.80	89
7	Pd-ZVI-400	400	12	0.040	15.24	95
8	Ni-ZVI-350	350	28	0.158	23.34	77
9	Ni-ZVI-370	370	21	0.090	16.59	90
10	Ni-ZVI-400	400	13	0.042	14.49	99
11	Ref.[c]		0.13-0.19	n.d.[b]	n.d.[b]	100

[a]Calculated from the following formula: Fe^0 content$=-51.387X^2+151.88X$, where X represents an intensity ratio of $D_{110}/(D_{110}+D_{311})$.
[b]Not determined.
[c]Commercial Fe^0 particles (Alfa, <10 micron).

acetylacetonate ($Pd(C_5H_7O_2)_2$, Sigma-Aldrich, 99%, Pd/Fe ratio=0.1 wt%) or nickel chloride hexahydrate ($NiCl_2 \cdot 6H_2O$, Kanto Chemical, 97%, Ni/Fe ratio=1 wt%) was first dissolved in 35 mL of ethanol, followed by the addition of the iron salt. The physical properties of Pd-ZVI and Ni-ZVI aerogels reduced at different temperatures are summarized in Table 1 (entries 5-7 for Pd-ZVI aerogels and entries 8-10 for Ni-ZVI aerogels).

3. Characterizations

N_2 adsorption-desorption analysis was performed by using a Micromeritics ASAP 2010. Before measurement, all ZVI aerogels were dried under vacuum at 120 °C overnight and subsequently purged with He. Temperature-programmed reduction (TPR) analysis was also done with a sample of 0.03 g, where the hydrogen consumption was monitored by using a GC with thermal conductivity detector (TCD). The samples were heated from 27 °C to 627 °C at a ramping rate of 1 °C/min under 4% H_2/Ar with a flow rate of 30 mL/min.

X-ray diffraction (XRD) patterns of ZVI aerogels were collected with a Rigaku D/Max-2500 diffractometer (Cu-K_α source, λ=0.1541 nm) with a step size of 0.02° in the 2θ range of 5° to 90°. The content of Fe^0 in the aerogels was calculated according to the relational formula between the diffraction intensity, D_{110}, of (110) plane of Fe^0, the diffraction intensity, D_{311}, of (311) plane of magnetite, the mixing ratios based on the measured patterns, which is described in the literature [13]. The relational formula is expressed as follows:

$$Fe^0 \text{ content} = -51.387X^2 + 151.88X$$

where X represents an intensity ratio of $D_{110}/(D_{110}+D_{311})$. Transmission electron microscopy (TEM) images were also obtained with a Philips CM-30 instrument operated at 50-300 kV.

4. TCE Dechlorination

TCE dechlorination was conducted in 2 mL septum vial with no headspace, where Fe concentration was 10 g/L. The experiment was initiated by adding 5 μL of TCE stock solution by a gastight syringe, which resulted in initial TCE concentration of 5 mg/L in the case of ZVI aerogels. For Pd-ZVI and Ni-ZVI aerogels, the initial TCE concentration was 50 mg/L. The reaction vials were then stirred in a shaking incubator (200 rpm) at 20 °C under dark. Prior to all experiments, distilled water was purged with N_2 for 2 h.

After ZVI aerogels were collected by placing a magnet at the bottom of vial at a certain time, 1 mL of supernatant was withdrawn and extracted with 3 mL of *n*-hexane (Sigma-Aldrich, >99%). The TCE concentration was finally analyzed with an HP6890 gas chromatograph (GC) equipped with an HP-1 column and an electron capture detector (ECD).

RESULTS

The dechlorination of TCE with the initial concentration of 5 mg/L was carried out by using the commercial ZVI sample (Alfa, 0.13-0.19 m^2/g; entry 11 in Table 1) and ZVI aerogels reduced at different temperatures in the range of 350-500 °C. As shown in Fig. 1a, the TCE conversion on the former was about 10.7% at s reaction time of 32 h, whereas all ZVI aerogels showed much higher TCE conversion at our reaction conditions. Especially, ZVI-370 aerogel decomposed TCE completely within 11 h, where reaction intermediates such as DCE and VC were not detected at all during the reaction course. On the basis of the normalized TCE concentrations (C/C_0) shown in Fig. 1a, the initial rate constants ($k_{initial}$) of ZVI aerogels were calculated, assuming that TCE dechlorination has a pseudo first-order reaction rate. As a result, ZVI-370 aerogel achieved $k_{initial}$ (~0.240 h^{-1}), which is 4.4 and 7.5 times higher than the rate constants of ZVI-400 ($k_{initial}$=0.055 h^{-1}) and ZVI-500 ($k_{initial}$=0.032 h^{-1}) aerogels, respectively (*cf.* Fig. 1b).

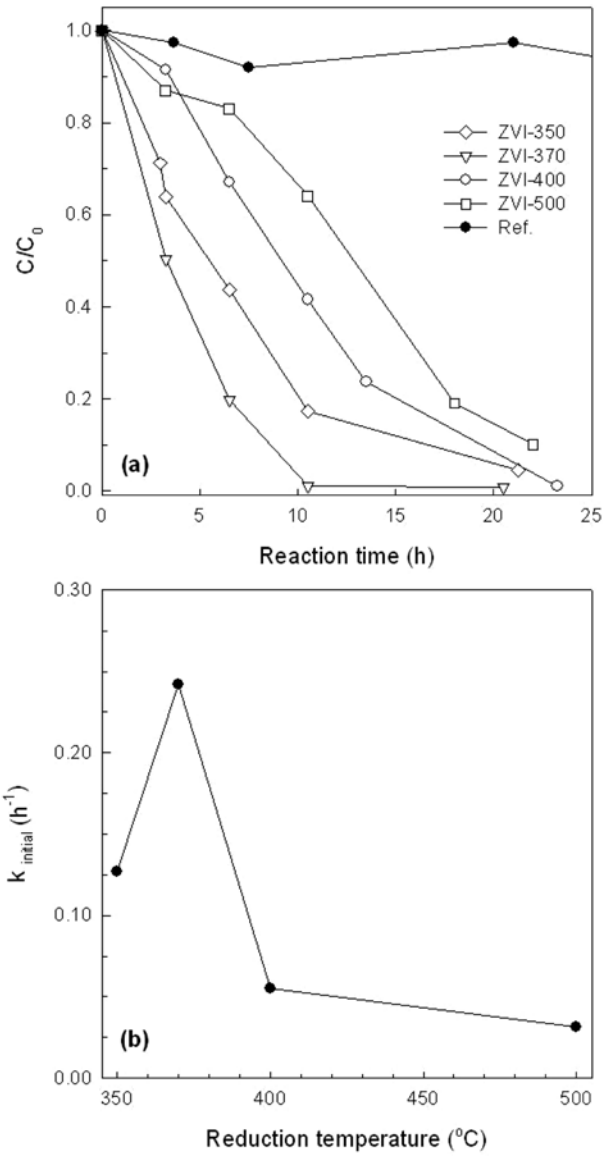

Fig. 1. Normalized TCE concentration as a function of reaction time on ZVI aerogels reduced at various temperatures (a) and their pseudo first-order rate constant (b).

On the other hand, bimetallic Pd-ZVI aerogels (Pd/Fe ratio=0.1 wt%) and Ni-ZVI aerogels (Ni/Fe ratio=1 wt%) were tested in TCE dechlorination, where the initial TCE concentration was 50 mg/L, due to the expected higher reaction rate by metal additives. As shown in Fig. 2, a complete TCE dechlorination was observed on Pd- ($k_{initial}$ =3.4-5.3 h^{-1}) and Ni-ZVI aerogels ($k_{initial}$=0.61-0.82 h^{-1}) reduced at lower temperatures such as 350 or 370 °C within 30 min and 2 h, respectively. Since the amount of Pd in Pd-ZVI aerogels (0.1 wt%) is much lower than that of Ni in Ni-ZVI aerogels (1 wt%), the Pd activity was much higher than the Ni activity in TCE dechlorination.

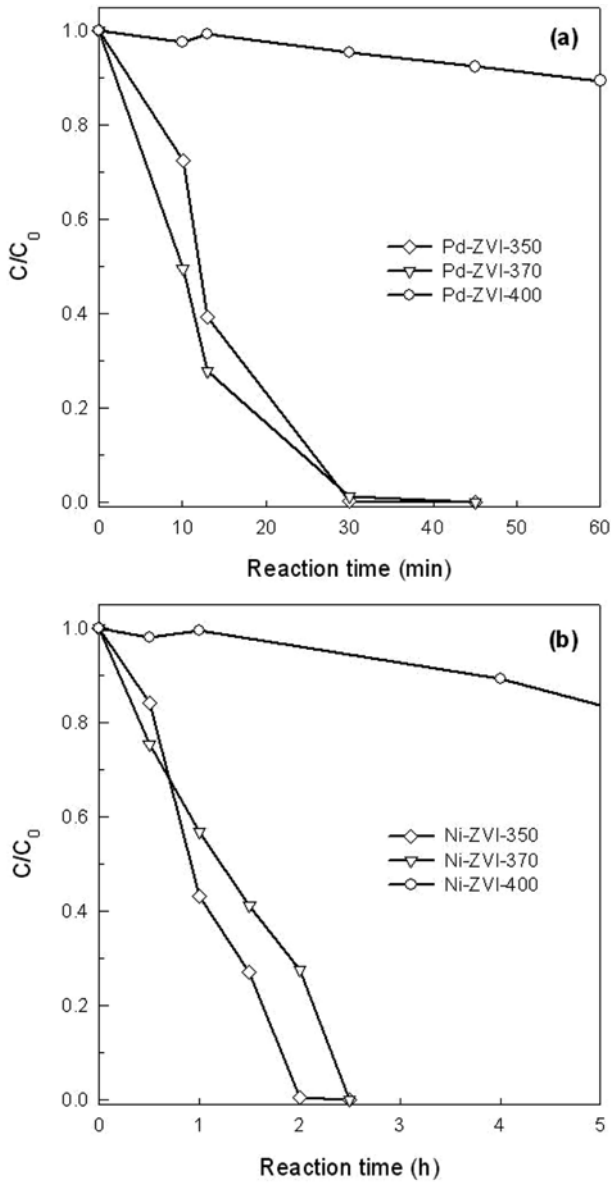

Fig. 2. Normalized TCE concentration as a function of reaction time on Pd- (a) and Ni-ZVI aerogels (b) reduced at 350 (◇), 370 (▽), and 400 °C (○).

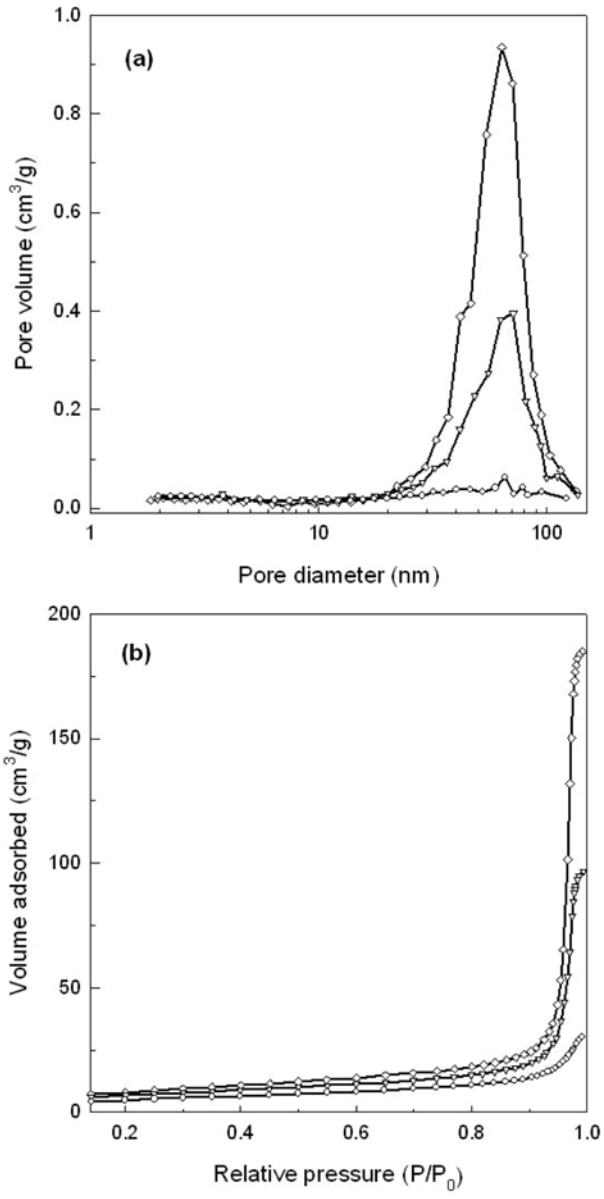

Fig. 3. Pore size distributions (a) and isotherms (b) of ZVI aerogels reduced at 350 (◇), 370 (▽), and 400 °C (○).

This is supported by the result that faster degradation was observed on Pd-ZVI-400 aerogel than on Ni-ZVI-400 aerogel, although both aerogels showed lower TCE degradation rates than Pd- and Ni-ZVI aerogels reduced at 350 and 370 °C.

DISCUSSION

1. ZVI Aerogels on TCE Dechlorination

As summarized in Table 1 and Fig. 3, the BET surface areas and total pore volumes of ZVI aerogels decreased with reduction temperature increasing to 500 °C because thermal treatment at higher temperatures leads to the agglomeration of iron particles. ZVI aerogel particles reduced at 350 and 370 °C showed uniform size distribution and small average particle size (30-40 nm). In all cases, the number of large particles increased with the reduction temperature. However, as reduction temperature goes down, the extent of such an increase in the BET surface area is smaller than that of an increase in the TCE dechlorination rate constant ($k_{initial}$). For example, the BET surface area (25 m^2/g) of ZVI-370 aerogel is 1.3 and 4.2 times higher than that of ZVI-400 (19 m^2/g) and ZVI-500 (6 m^2/g) aerogels, respectively, whereas $k_{initial}$ of the former aerogel is 4.4 and 7.5 times higher than that of the latter aerogels. This clearly indicates that the TCE dechlorination rate is not linearly correlated with the surface area of ZVI aerogel, which is confirmed by the observation that $k_{initial}$ of ZVI-370 aerogel is 2-fold higher than that of ZVI-350 aerogel, although the difference in the BET surface area of both ZVI aerogels is only 5 m^2/g. Therefore, it can be considered that the TCE dechlorination activities of ZVI aerogels would be enhanced by other parameters, in addition to their surface areas.

Hence, we investigated the compositions of ZVI aerogels reduced

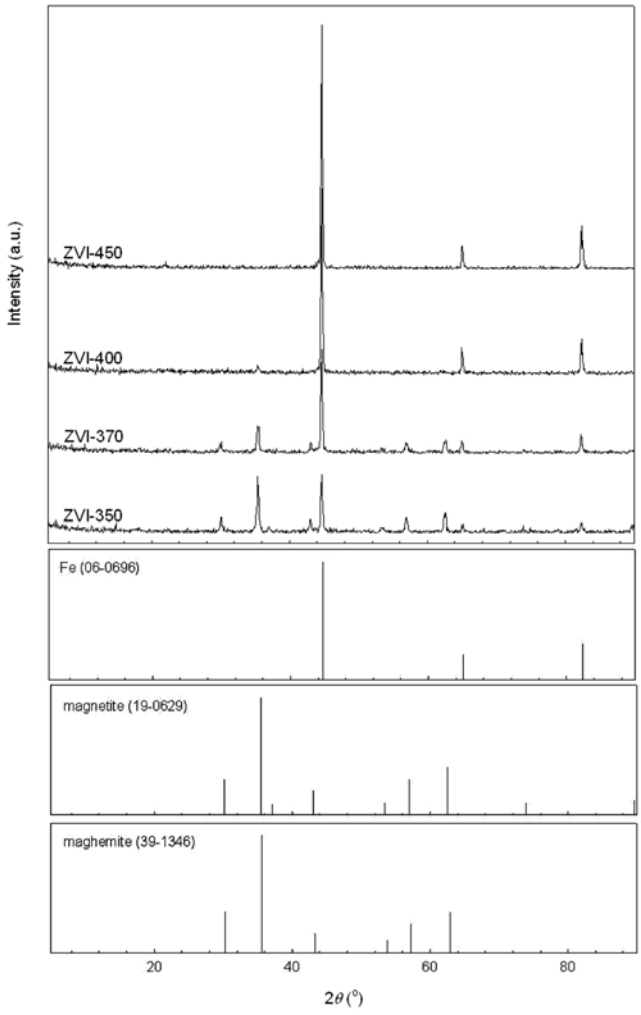

Fig. 4. XRD patterns of ZVI aerogels reduced at 350, 370, 400, and 450 °C, and reference data of Fe_0, magnetite, and maghemite from the JCPDS.

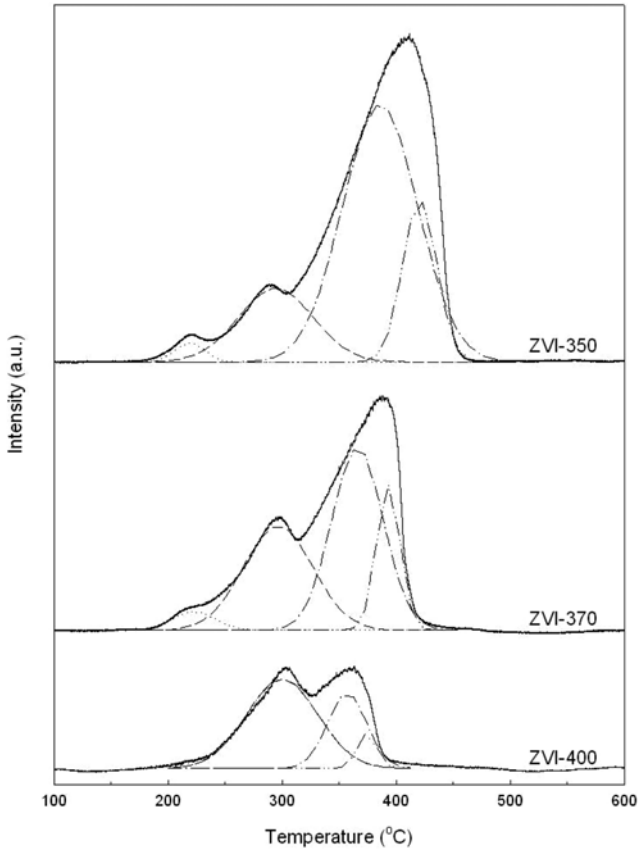

Fig. 5. TPR profiles of ZVI aerogels reduced at 350, 370, and 400 °C.

at different temperatures from their XRD patterns. As shown in Fig. 4, ZVI aerogels reduced at higher temperatures than 400 °C were mostly Fe^0 (>97%) whereas reduction at 350 and 370 °C produced a mixture of metallic iron and iron oxide(s) (FeO_x), indicating that lower reduction temperature leads to incomplete transition of iron oxide aerogels to metallic iron. The FeO_x was assigned as magnetite (Fe_3O_4) and/or maghemite (γ-Fe_2O_3), which cannot be clearly distinguished. As expected, the FeO_x content increased up to 36% with decreasing reduction temperature. From these XRD data and the experimental results on TCE dechlorination, it can be suggested that the mixture of Fe^0 and FeO_x has a favorable effect on TCE dechlorination rather than a single Fe^0; e.g., ZVI-370 aerogel, showing that the highest TCE dechlorination rate in the conditions employed in this study, is composed of ~87% Fe^0 and ~13% FeO_x. However, more FeO_x in ZVI aerogels is not beneficial for TCE dechlorination because ZVI-350 aerogel containing more FeO_x (~36%) and less Fe^0 (~74%) than ZVI-370 aerogel dechlorinated TCE in lower amounts. This is due to the smaller amount of the active metal center, Fe^0. It is, hence, necessary to investigate which iron oxide exists in ZVI aerogels, since magnetite (or maghemite) is electrically conductive (or non-conductive).

Fig. 5 shows the TPR profiles obtained by using ZVI aerogels reduced at 350, 370, and 400 °C. Note that all ZVI aerogels were finally treated in 1% O_2/N_2 at room temperature for 1 h, prior to the exposure to the air. The TPR profile of ZVI-400 aerogel is composed of two peaks observed in the range of 250-400 °C. In general, it is suggested that the reduction of Fe_2O_3 to metallic iron proceeds in two steps via Fe_3O_4 intermediate [22,23], as follows:

$$3Fe_2O_3+H_2 \rightarrow 2Fe_3O_4+H_2O \quad (5)$$

$$Fe_3O_4+4H_2 \rightarrow 3Fe+4H_2O \quad (6)$$

thus indicating that the final peak in TPR profiles of ZVI aerogels corresponds to H_2 consumption attributed to the Fe_3O_4-to-Fe^0 transition. On the other hand, Carpenter et al. [24] reported that, when treated in argon at 260 °C, the iron oxide aerogel of a spinel structure is an intermediate between Fe_3O_4 and γ-Fe_2O_3, that is, a partially-oxidized magnetite, whereas the thermal treatment in air produced maghemite with slightly larger particles. It can be, therefore, considered that ZVI-400 aerogel contains an amorphous layer of partially oxidized magnetite at the ZVI surface produced by O_2 treatment at RT since the XRD pattern of ZVI-400 aerogel showed no indication of iron oxide(s). Accordingly, the reduction process of ZVI-400 aerogel is composed of the first reduction of the amorphous partially oxidized magnetite layer to Fe_3O_4 and its subsequent reduction to Fe^0. This is supported by the result that the peak areas obtained by fitting curves are both similar.

In comparison with the TPR profiles of ZVI aerogels reduced at different temperatures, there are three distinct observations. The first is related to the similar areas of TPR peak corresponding to the reduction of the amorphous partially oxidized magnetite layer to Fe_3O_4, irrespective of reduction temperature. This indicates that the iron oxide layer exists in similar amounts at ZVI aerogels reduced in the temperature range of 350-400 °C due to weak O_2 passivation. The second observation is that, as reduction temperature decreased to 350 °C, the area of final TPR peak was getting much higher, meaning that the amount of Fe_3O_4 (magnetite) present in ZVI aerogels increases with reduction temperature decreasing. In addition, the TPR peak shown at the maximum temperature of ~220 °C was observed in the largest on ZVI-350 aerogel. This peak can be ascribed to the Fe_2O_3-to-Fe_3O_4 transition, since the reduction of Fe_2O_3 has been reported to be carried out at lower temperature than that of Fe_3O_4 [22,23]. Therefore, as reduction temperature decreases, the higher content of maghemite, which the phase of Fe_2O_3 is assumed to be in case of ZVI aerogels from XRD data shown in Fig. 4, exists and further lowers the catalytic activity of ZVI aerogels on TCE dechlorination because non electron-conducting maghemite inhibits electron transfer from Fe^0. However, it was not considered that the difference in low-temperature TPR peak areas between ZVI-350 and ZVI-370 aerogels is as much as that in the TCE dechlorination rate constants of both aerogels. From these considerations, the Fe^0 content rather than the content of iron oxides (maghemite and magnetite) is believed to bring about the difference in the TCE dechlorination rate constants of ZVI-350 and ZVI-370 aerogels, even though the existence of magnetite is, indeed, of advantage for TCE dechlorination. Hence, there is one thing left, that is, where these oxides are present that should be understood to make clear which roles they are playing in TCE dechlorination.

The structure of ZVI aerogels reduced at different temperatures was characterized by TEM analysis. It was shown in Fig. 6 that the layer of iron oxide(s) confirmed by EDX analysis was coated at the outer surface of particles, where the layer thickness is very similar in all ZVI aerogels. Therefore, such an oxide layer is considered to be produced by O_2 treatment at room temperature, which is in agreement with TPR data described above. Fig. 6 also shows that ZVI aerogel particles become bigger and more aggregated with reduction temperature increasing to 400 °C. In particular, the core of ZVI aerogel particles appears to be homogeneous. This indicates that iron oxides (maghemite and/or magnetite) and Fe^0 are homogeneously mixed inside the particle cores, which is caused by the fact that iron oxide aerogels retain the pore structure. It is, therefore, considered that ZVI aerogels containing more iron oxides and less Fe^0 inside each particle were produced by H_2 reduction at lower tem-

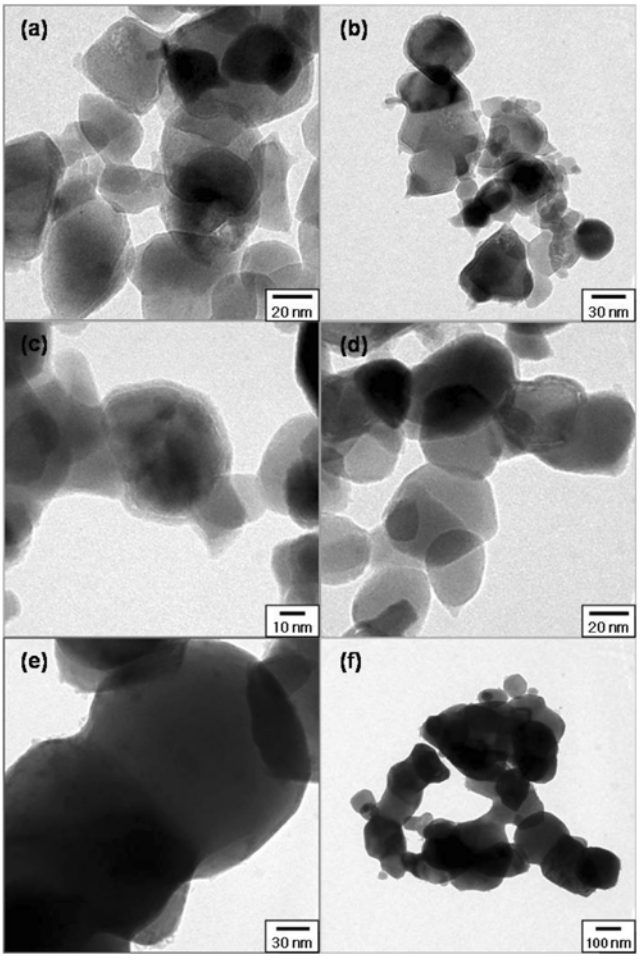

Fig. 6. TEM images of ZVI aerogels reduced at 350 (a, b), 370 (c, d), and 400 °C (e, f).

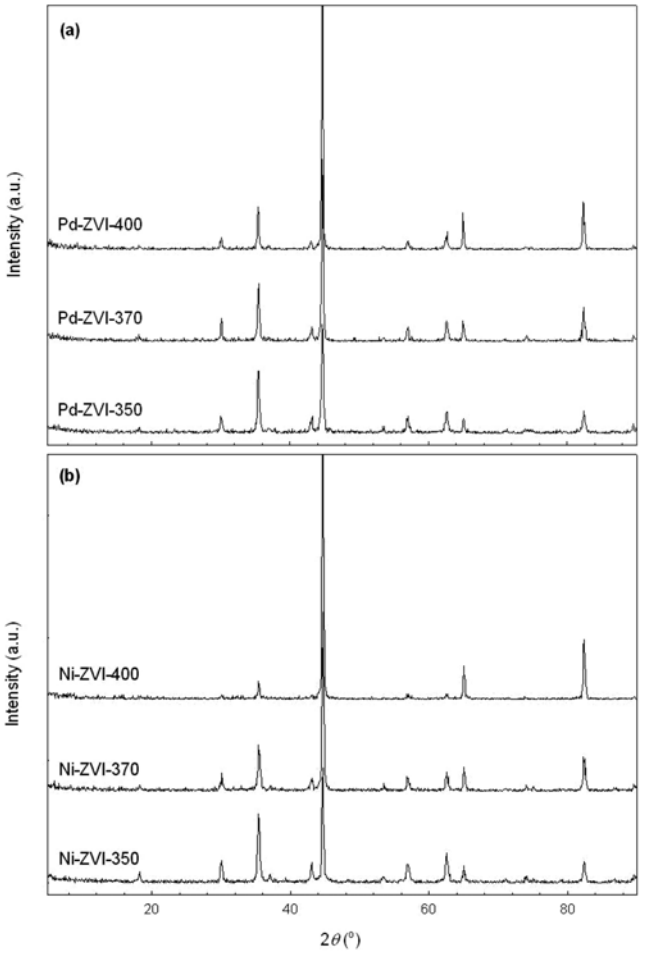

Fig. 7. XRD patterns of Pd- (a) and Ni-ZVI aerogels (b) reduced at 350, 370, and 400 °C.

peratures on the basis of the observation that, as reduction temperature decreased, both amounts of maghemite and magnetite increased whereas the Fe^0 content decreased. It is, finally, concluded that the reduction at 370 °C produced ZVI aerogel particles homogeneously composed of both Fe^0 (~87%) and FeO_x (~13%) in an adequate amount ratio, resulting in higher TCE dechlorination rate.

2. Pd- and Ni-ZVI Aerogels on TCE Dechlorination

When Pd- and Ni-ZVI aerogels were applied for TCE dechlorination, the effect of reduction temperature was similar to the one obtained from ZVI aerogels. With reduction temperature decreasing to 350 °C, a mixture of Fe^0 and FeO_x was found in Pd- and Ni-ZVI aerogels, as shown in Table 1 and Fig. 7. In particular, the Fe^0 contents (77-78%) in Pd-ZVI-350 and Ni-ZVI-350 aerogels were observed to be higher than that in ZVI-350 aerogel (64%), indicating that the addition of Pd and Ni to ZVI aerogels facilitates the reduction of iron oxide aerogels due to faster hydrogen adsorption of both additives. There was, however, little difference in Fe^0 content between Pd- or Ni-ZVI and ZVI aerogels when reduced at higher temperatures than 370 °C. Additionally, it is interesting to note that XRD patterns of Pd- and Ni-ZVI aerogels reduced at 350 and 370 °C clearly showed the peaks at 18.2° and 89.6°, which is characteristic of magnetite but not maghemite. This indicates that Fe_3O_4 and Fe^0 co-exist homogeneously inside the particle cores of Pd- and Ni-ZVI aerogels. On the other hand, the iron oxide layer can be also identified to exist in the outer surface of Pd- and Ni-ZVI aerogels from TEM images shown in Figs. 8 and 9, which is similar to ZVI aerogels. In summary, when Pd or Ni is added to ZVI aerogels, a reduction at 350 and 370 °C leads to the production of Pd- or Ni-ZVI aerogel particles in which both Fe^0 and Fe_3O_4 co-exist homogeneously, of which both are advantageous in TCE dechlorination. Hence, Pd- and Ni-ZVI aerogels reduced at 350 °C showed TCE dechlorination activities comparable to those of both aerogels reduced at 370 °C, although the former aerogels have less Fe^0 content.

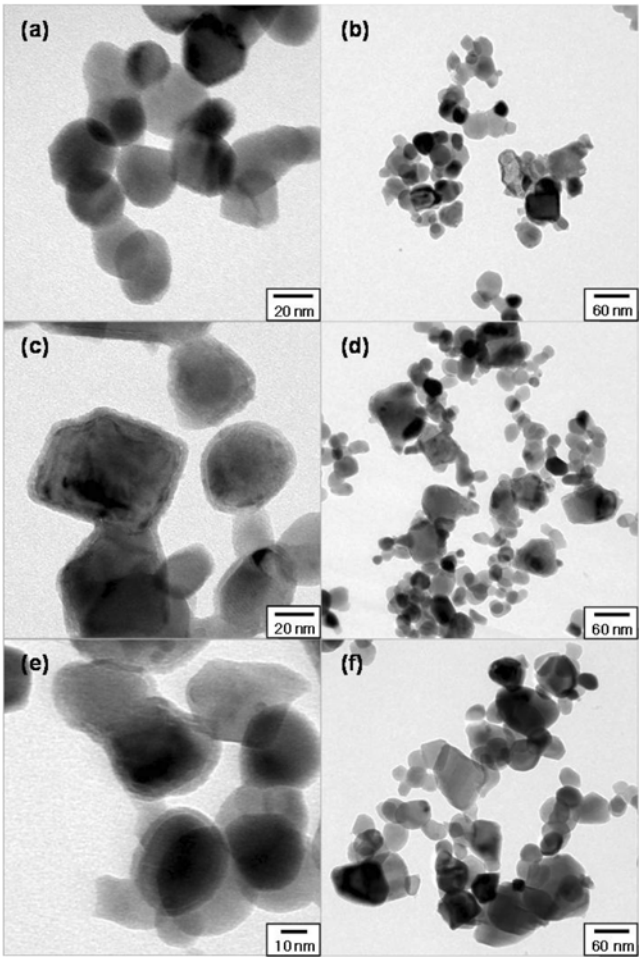

Fig. 8. TEM images of Pd-ZVI aerogels reduced at 350 (a, b), 370 (c, d), and 400 °C (e, f).

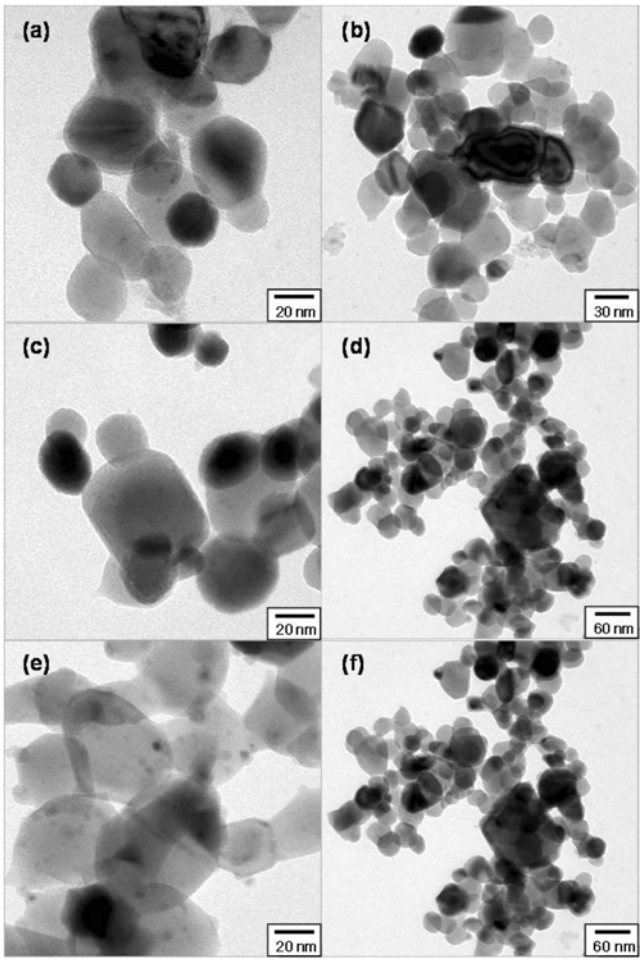

Fig. 9. TEM images of Ni-ZVI aerogels reduced at 350 (a, b), 370 (c, d), and 400 °C (e, f).

CONCLUSIONS

We have investigated the effect of reduction temperature in preparing ZVI aerogels for TCE dechlorination. As expected, a reduction at lower temperatures led to the formation of ZVI aerogels with higher surface areas and less Fe^0 content. However, the highest TCE dechlorination rate constant was obtained by using ZVI aerogels reduced at 370-380 °C which have BET surface area of 25 m^2/g and Fe^0 content of 87%. This suggests that the TCE dechlorination rate is not linearly correlated with the surface area of ZVI aerogel. It was then found in XRD, TPR, and TEM characterization data that ZVI-350 and ZVI-370 aerogel particles with a partially oxidized mag-

netite layer consist of both Fe^0 and FeO_x in the cores of each particle in a different amount ratio, where FeO_x is a mixture of maghemite and magnetite. Especially, higher Fe^0 composition in the particles was observed in ZVI-370 aerogel than in ZVI-350 aerogel. From this result, it can be considered that the amount ratio of Fe^0 and FeO_x components in ZVI aerogel particles depends on reduction temperature. Consequently, the amount ratio of Fe^0/FeO_x observed in ZVI-370 aerogel would be optimal for TCE dechlorination in our experimental conditions since ZVI-370 aerogel showed the highest TCE dechlorination rate.

Also, a similar effect of reduction temperature was observed by using Pd- and Ni-ZVI aerogels prepared via cogellation. However, both Fe^0 and Fe_3O_4 were found to co-exist homogeneously in the cores of these aerogel particles, where the amount ratio of Fe^0/Fe_3O_4 is different between Pd(or Ni)-ZVI-350 and Pd(or Ni)-ZVI-370 aerogels. Since Fe^0 and Fe_3O_4 components are both effective for TCE dechlorination although their TCE dechlorination activities are different from each other, the activities of Pd-ZVI-350 and Ni-ZVI-350 aerogels were comparable to those of Pd-ZVI-370 and Ni-ZVI-370 aerogels, respectively. Therefore, in case of Pd- and Ni-ZVI aerogels, a reduction at lower temperatures leads to the preferable formation of Fe_3O_4 in addition to faster reduction of iron oxide aerogels, resulting in enhanced TCE dechlorination rate.

REFERENCES

1. C. M. Kao, S. C. Chen and J. K. Liu, *Chemosphere*, **43**, 1071 (2001).
2. M. M. Scherer, S. Richter, R. L. Valentine and P. J. J. Alvarez, *Critical Reviews in Environmental Science and Technology*, **30**(3), 363 (2000).
3. D. E. Meyer and D. Bhattacharyya, *J. Phys. Chem. B*, **111**, 7142 (2007).
4. S. M. Ponder, J. G. Darab and T. E. Mallouk, *Environ. Sci. Technol*., **34**, 2564 (2000).
5. S. M. Ponder, J. G. Darab, J. Bucher, D. Caulder, I. Craig, L. Davis, N. Edelstein, W. Lukens, H. Nitsche, L. Rao, D. K. Shuh and T. E. Mallouk, *Chem. Mater*., **13**, 479 (2001).
6. B. Schrick, J. L. Blough, A. D. Jones and T. E. Mallouk, *Chem. Mater.*, **14**, 5140 (2002).
7. C. B. Wang and W. X. Zhang, *Environ. Sci. Technol*., **31**, 2154 (1997).
8. J. T. Nurmi, P. G. Tratnyek, V. Sarathy, D. R. Baer, J. E. Amonette, K. Pecher, C. Wang, J. C. Linehan, D. W. Matson, R. L. Penn and M. D. Driessen, *Environ. Sci. Technol*., **39**, 1221 (2005).
9. G. N. Glavee, K. J. Klabunde, C. M. Sorensen and G. C. Hadjipanayis, *Inorg. Chem.*, **34**, 28 (1995).
10. N. Duxin, O. Stephan, C. Petit, P. Bonville, C. Colliex and M. P. Pileni, *Chem. Mater.*, **9**, 2096 (1997).
11. N. Duxin, M. P. Pileni, W. Wernsdorfer, B. Barbara, A. Benoit and D. Mailly, *Langmuir*, **16**, 11 (2000).
12. E. E. Carpenter, S. Calvin, R. M. Stroud and V. G. Harris, *Chem. Mater.*, **15**, 3245 (2003).
13. M. Uegami, J. Kawano, T. Okita, Y. Fujii, K. Okinaka, K. Kakuya and S. Yatagai, US Patent 7,022,256 (2006).
14. Y. Liu, H. Choi, D. Dionysiou and G. V. Lowry, *Chem. Mater*., **17**, 5315 (2005).
15. P. D. Mackenzie, D. P. Horney and T. M. Sivavec, *J. Hazard. Mater.*, **68**, 1 (1999).
16. C.-C. Liu, D.-H. Tseng and C.-Y. Wang, *J. Hazard. Mater. B*, **136**, 706 (2006).
17. T. L. Johnson, W. Fish, Y. A. Gorby and P. G. Tratnyek, *J. Contam. Hydrol.*, **29**, 379 (1998).
18. A. G. B. Williams and M. M. Scherer, *Environ. Sci. Technol*., **38**, 4782 (2004).
19. W. X. Zhang, C. B. Wang and H. L. Lien, *Cata. Today*, **40**(4), 387 (1998).
20. E. K. Nyer and D. B. Vance, *Ground Water Monit. Rem*., **21**(2), 41 (2001).
21. A. E. Gash, T. M. Tillotson, J. H. Satcher Jr., J. F. Poco, L. W. Hrubesh and R. L. Simpson, *Chem. Mater*., **13**, 999 (2001).
22. O. J. Wimmers, P. Arnoldy and J. A. Moulijn, *J. Phys. Chem*., **90**, 1331 (1986).
23. M. J. Tiernan, P. A. Barnes and G. M. B. Parkes, *J. Phys. Chem*., **105**, 220 (2001).
24. E. E. Carpenter, J. W. Long, D. R. Rolison, M. S. Logan, K. Pettigrew, R. M. Stroud, L. T. Kuhn, B. R. Hansen and S. Morup, *J. Appl. Phys*., **99**, 08N711 (2006).